IEEE Access
Multidisciplinary | Rapid Review | Open Access Journal

Received May 9, 2019, accepted May 25, 2019, date of publication June 4, 2019, date of current version June 27, 2019.

Digital Object Identifier 10.1109/ACCESS.2019.2919729

Improvement of Optical and Thermal Properties for Quantum Dots WLEDs by Controlling Layer Location

YONG TANG, HANGUANG LU, JIASHENG LI, ZONGTAO LI, XUEWEI DU, XINRUI DING, AND BINHAI YU

Engineering Research Centre of Green Manufacturing for Energy-Saving and NewEnergy Technology, School of Mechanical and Automotive Engineering, South China University of Technology, Guangzhou 510640, China

Corresponding author: Zongtao Li (meztli@scut.edu.cn)

This work was supported in part by the National Natural Science Foundation of China under Grant 51735004 and Grant 51775199, and in part by the Natural Science Foundation of Guangdong Province under Grant 2014A030312017 and Grant 2017B010115001.

ABSTRACT The inorganic halide perovskite quantum dots (QDs) have been considered as a promising substitute for white light-emitting diodes (WLEDs). In this paper, the green $CsPbBr_3$ QDs and red $K_2SiF_6:Mn^{4+}$ (KSF) phosphor were used to fabricate the conversion layers. Because the location of the layers is fundamental to the absorption priority of blue light, the location of KSF and QDs were controlled and the QDs-up type and QDs-down type WLEDs were made. The optical power, luminous efficiency, CCE, and luminous intensity in the middle of QDs-up type are 13.83 mW, 13.54 lm/W, 11.94%, and 2.65 cd, meaning 24.26%, 25.72%, 2.63%, and 23.83% higher than those of QDs-down type, respectively. In addition, the QDs-up type has a lower correlated color temperature (CCT) shift of 734 K and a decreased highest temperature of 56.8° (51.5% and 14.9% lower). These key property differences indicate that the QDs-up type is more suitable for the application in display and backlight. In order to explore the reasons for these differences, the emission spectra, CCE, reflection rate, absorption rate, and temperature curves of QDs or KSF films were also analyzed, which provided a better understanding of designing package structures.

INDEX TERMS Quantum dots WLEDs, optical properties, thermal properties, layer location.

I. INTRODUCTION

White light-emitting diodes (WLEDs) are rapidly replacing traditional light sources, because of their high luminous flux, low energy consumption, low cost, environmentally friendly qualities, etc. [1]–[4] For attaining a wide color. gamut and controlling the correlated color temperature (CCT), green and red phosphors are conventionally used [5] Because they contain rare-earth elements, the growing phosphor consumption will increase product costs and reduce the availability of WLEDs [6], [7]. Also, phosphor has difficulties in gaining a breakthrough in color gamut and an adjustable CCT for display usage [8]–[10]. Therefore, new luminescent materials need to be used in a WLEDs, as a substitute for phosphor.

As inorganic lead halide perovskite quantum dots (QDs), $CsPbX_3$ (X = Cl, Br, I) QDs become promising fluorescence material for fluorescent layers of WLEDs [11], [12]. They have narrow emission full width at half maximum (FWHM) (12-42 nm), broad wavelength coverage (400-700 nm), simplicity of modification and stable photochemical property. [13]–[17] In 2016, Li et al. used green $CsPbBr_3$ and red $CsPbI_3$ as the conversion layer, and different CCTs were attained by changing the ratio between red and green QDs [18] In the same year, Meyns' team introduced poly (maleic anyhdride-alt-1-octadenece) to synthesize green $CsPbBr_3$ and red $CsPbBr_{1.6}I_{1.4}$, which were then employed over a blue LED to obtain white light [19] Wei et al. packed green $CsPbBr_3$ and red $CsPb(Br_{0.4}I_{0.6})_3$ into crosslinked polystyrene (PS), and then combined them to prepare WLEDs [20] The perovskite QDs have a high color purity due to their narrow FWHM. However, the red perovskite QDs contained iodine are unstable at present, so the $CsPbBr_3$ QDs and commercial $K_2SiF_6:Mn^{4+}$ (KSF) were used in this article, to attain a wide color gamut for the display and backlight application [21], [22].

The associate editor coordinating the review of this manuscript and approving it for publication was Jiajie Fan.

In addition, the spatial distribution of luminescent materials plays an important role in the thermal performance and extraction efficiency for WLEDs illumination [23]–[27]. In 2015, Chiang et al. adjust the red and yellow phosphor layers to promote the luminous efficiency [27] By change the CdSe QDs position, Bin's team enhance the color rendering index from 57 to 92, and lower the temperature of WLEDs [28] But the influences of inorganic perovskite QDs layer location on optical and thermal properties have not been taken into consideration, especially for backlight and display.

In this study, for acquiring a better backlight and display, the fluorescent layer contained $CsPbBr_3$ QDs or red $K_2SiF_6:Mn^{4+}$ (KSF) phosphor were used. The location of QDs and KSF affects their absorption priority of blue light, and the reflectance rate and absorption rate of the below layer affect the color conversion of the above layer [29]. Thence, the QDs-up type and QDs-down type WLEDs were fabricated and the optical and thermal properties of two types differ greatly. For the usage in display and backlight, the main parameters conclude chromaticity coordinate, optical power, luminous efficiency, color conversion efficiency (CCE), luminous intensity, correlated color temperature (CCT) and its shift, working temperature and the color gamut. Based on the emission spectra, temperature curves and other measurement, the QDs-up type has a higher optical power by 24.26% and a higher luminous efficiency of 25.72%, an increased color conversion efficiency (CCE) by 2.63%, a higher luminous intensity by 23.83%, a lower correlated color temperature (CCT) shift by 51.5%, a decreased highest temperature by 14.9% and a similar color gamut. These results suggesting that the QDs-up type is more suitable for the LED backlight and display. After the analysis on the spectra, CCE, reflection rate, absorption rate, and thermal images of QDs or KSF films, the reasons why the QDs-up type has superior properties were clarified.

II. EXPERIMENTS

A. PREPARATION OF WLEDs WITH QDs AND KSF

The first synthesis of $CsPbBr_3$ QDs were reported previously [30]. The $CsPbBr_3$ QDs and KSF were dispersed in polydimethylsiloxane (PDMS) and then injected into a mold. After being heated at 90° C for 1 h, the thin films with green emission and red emission were made. To prepare an WLEDs, the blue LED was chosen as the excitation source of the $CsPbBr_3$ QDs and KSF. In this study, two types of excitation method are compared—the QDs-up type and QDs-down type—as shown in Figure 1a-c. The QDs film was located above the KSF film in QDs-up type, whereas the QDs-down type has the QDs distributed in the below film. It is necessary to attain similar chromaticity coordinates for comparing the properties of these two types WLEDs. Therefore, the concentrations of QDs and KSF were adjusting. The weight ratios of QDs in the thin film were set as 0.5%, 1%, 1.5%, 2% and 2.5%, and these of KSF were 12.5%, 15%, 25%, 35% and 50%. As shown in Figure 2 and Table 1, the QDs-up type with

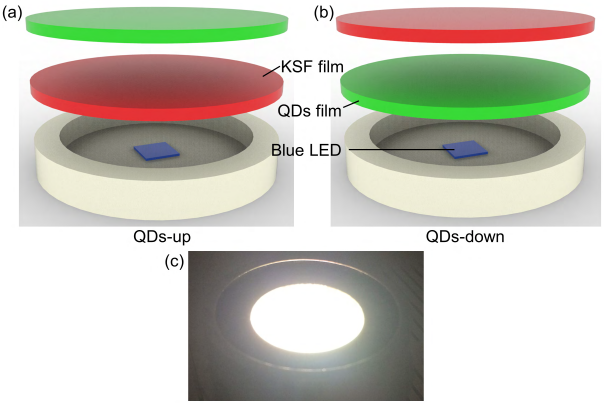

FIGURE 1. Schematic diagram of (a) the QDs-up type WLEDs and (b) the QDs-down type WLEDs; (c) photograph of the WLEDs.

TABLE 1. The concentration and Chromaticity coordinates of QDs and KSF in two types.

Name	QDs-up type	QDs-down type
Concentration of QDs	2%	1%
Concentration of KSF	12.5%	35%
Chromaticity coordinate (x)	0.3245	0.3466
Chromaticity coordinate (y)	0.3089	0.3372

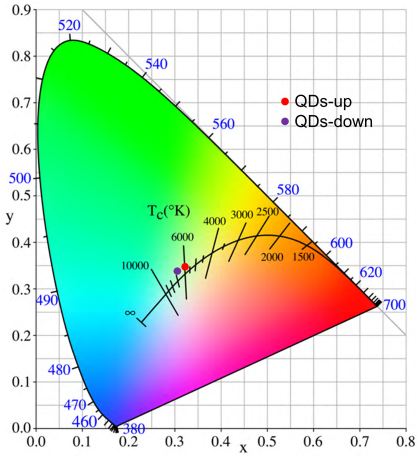

FIGURE 2. Chromaticity coordinates of two types WLEDs by concentration adjustment.

2% QDs and 12.5% KSF have a chromaticity coordinate of (0.3245, 0.3466). The chromaticity coordinate of QDs-down type with 1% QDs and 35% KSF is (0.3089, 0.3372). And the CCT of the QDs-up type and QDs-down type is 5848 K and 6657 K, respectively.

B. CHARACTERIZATIONS

The absorption spectra of the CsPbBr3 QDs, reflectance rate and absorption rate of QDs and KSF films were measured with a UV-vis spectrometer (UV-2700, Shimadzu, Japan). The photoluminescence spectra (PL spectra) were recorded by a fluorescence spectrophotometer (RF-6000, Shimadzu, Japan). The microscopic structure of the CsPbBr3 QDs

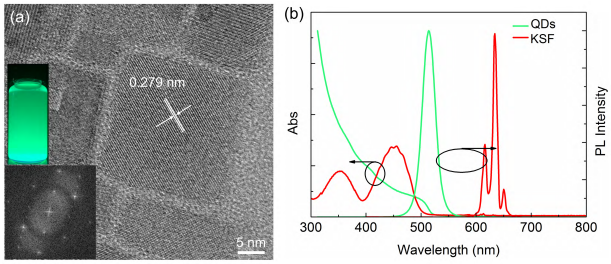

FIGURE 3. (a) TEM image, SAED and PL image of the $CsPbBr_3$ QDs; and (b) absorption spectra and PL spectra of QDs and KSF.

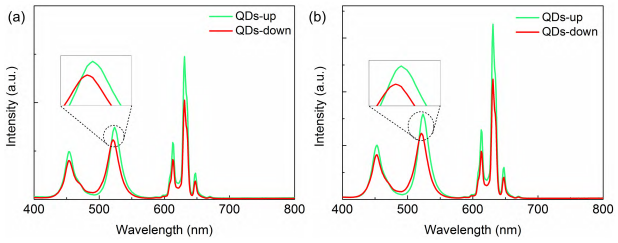

FIGURE 4. Emission spectra of QDs-up type and QDs-down type WLEDs (a) at 50 mA and (b) at 150 mA.

was collected by a transmission electron microscope (TEM, JEOL-2100F, Japan). The, emission spectra, luminous intensity and CCT of the WLEDs were obtained by an integrating sphere (Otsuka LE5400). With a thermal IR-camera (FLIR Therma CAM SC300), the thermal images and surface temperature were measured.

III. RESULT AND DISCUSSION

A. MORPHOLOGY AND SPECTRA OF QDs AND KSF

Figure 3a shows the TEM image, selected area electron diffraction (SAED), and PL image of the $CsPbBr_3$ QDs. From the TEM image, $CsPbBr_3$ QDs present an obvious cubic phase, so the distribution of crystals is relatively tidy. The SAED in the lower left corner indicates that the crystal plane spacing is 0.279 nm, which shows the good crystallinity of QDs. The absorption spectra and PL spectra in Figure 3b show some differences between QDs and KSF. First, the absorption peak of QDs is 502 nm, and the lower wavelength corresponds to the higher absorption value, whereas the two absorption peaks of KSF appear at 353 and 451 nm. The blue LED in the work has an emission peak at 450 nm, and both the QDs and KSF have absorption from 300 to 500 nm, so the green and red emission can be well generated. Second, the QDs have one peak, while KSF has three peaks in PL spectra, and the FWHM of the former is 28 nm and those of the latter is 9, 9, and 7 nm, respectively. Finally, the Stoke shift of QDs is 12 nm, while that of KSF is more than 160 nm. There is an overlapping between the absorption peak and emission peak of QDs, which implies the small reabsorption of QDs.1

B. COMPARISON OF OPTICAL PROPERTIES BETWEEN QDs-up TYPE AND QDs-down TYPE

The emission spectra of two types were first measured, as shown in Figure 4. The QDs-up type has a significantly stronger emission than that of the QDs-down type at different wavelengths. For blue, green and red emission, the peak values of QDs-up type are 23.31%, 13.58%, 43.30%, 44.10% and 43.97% higher than those of QDs-down type at 50 mA, respectively. Besides, the FWHMs of the two types WLEDs at 50 or 150 mA are the same, 18 nm for the blue emissions, 19 nm for the green emissions, 5, 9 and 5 nm for the red emissions. These narrow FWHMs proves the higher color purity of the WLEDs. To further understand the optical intensity differences, the optical power and CCE were attained based on the emission spectra.

The optical power was calculated by integration in emission spectra. However, the blue, green and red emissions cannot be integrated directly, because of the spectra overlap. Thence, we multiply the coefficients α and β. The α is defined as the ratio of peak intensity between the blue emission and blue LEDs. The β is defined as the ratio of peak intensity between the red KSF emission and a reference LED device without QDs. The green emission power can be attained by subtracting the blue and red emission power from the white light spectra. As a result, the blue emission power P_{B_em}, green emission power P_{G_em}, and red emission power P_{R_em} can be calculated as follows:

$$P_{B\_em} = \alpha \int_{\lambda_1}^{\lambda_2} S_{B\_ref}(\lambda) d\lambda, \tag{1}$$

$$P_{R\_em} = \beta \int_{\lambda_1}^{\lambda_2} S_{R\_ref}(\lambda) d\lambda, \tag{2}$$

$$P_{G\_em} = \int_{\lambda_1}^{\lambda_2} S(\lambda) d\lambda - P_{B\_em} - P_{R\_em}, \tag{3}$$

where $S_{B\_ref}(\lambda)$, $S_{R\_ref}(\lambda)$ and $S(\lambda)$ correspond to the emission spectra of the blue LED, reference LED device only with red KSF, and the two types WLEDs, respectively. The integrating wavelength range $[\lambda_1, \lambda_2]$ were as [360,830 nm]. The optical power results of three emissions and the whole LED device are shown in Figure 5. The separated emission power of LED devices without KSF films, and that without QDs films are shown in Figure 6c and d.

Figure 5a-d shows that with increased current, the optical power of QDs-up type increases with a near linear curve, but the slope in QDs-down type decreases and the disparity between them become more obvious. For the blue emission, the optical power of QDs-up type is 11.15% higher than that of the QDs-down type at 50 mA (Figure 5a). These differences are related to the blue emission intensity absorbed by QDs and KSF films. From Figure 6c and d, only a fraction of blue emission remains after passing through the QDs films. When the QDs distributed in the below film, most of the blue light is absorbed, and more KSF phosphor is needed. The high KSF concentration of 35% leads to a further absorption.

The QDs film in QDs-down type is closer to the blue LED. However, its optical power of green emission is 13.62% lower than that of the QDs-up type at 50 mA (Figure 5b).

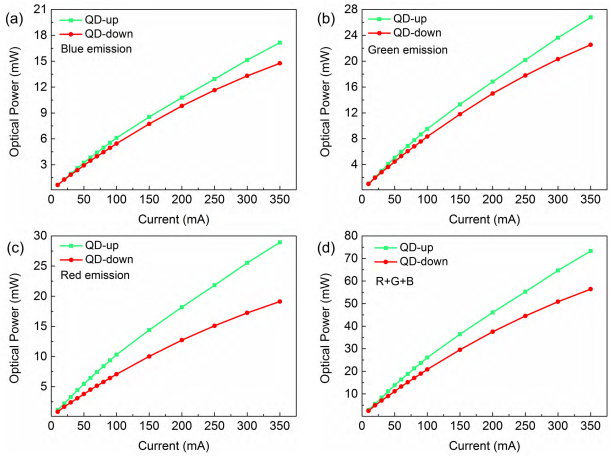

FIGURE 5. **(a) Optical power of the blue emission from blue LED with different currents; (b) optical power of the green emission from QDs with different currents; (c) Optical power of the red emission from KSF with different currents; and (d) optical power of the whole LED device with different currents.**

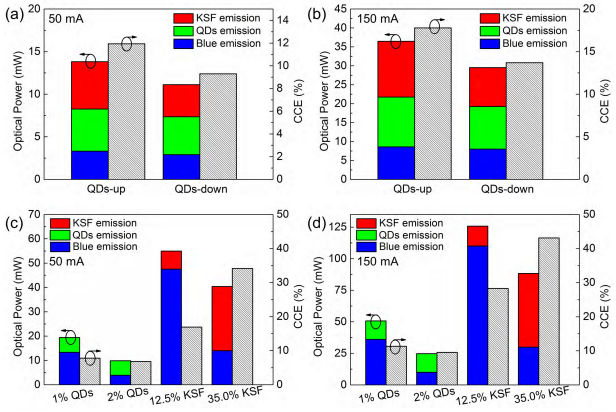

FIGURE 6. **Separated emission power and CCE of QDs-up type and QDs-down type WLEDs (a) at 50 mA and (b) at 150mA; separated emission power and CCE of LED devices without KSF film, and that without QDs film (c) at 50 mA and (d) at 150mA.**

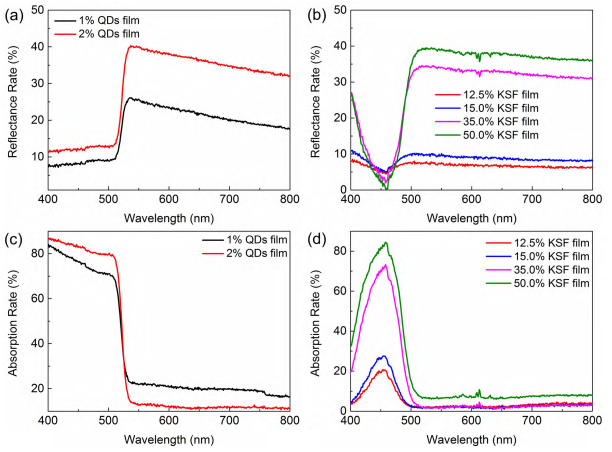

FIGURE 7. **Reflectance rate of (a) QDs films and (b) KSF films with different concentrations; absorption rate of (c) QDs films and (d) KSF films with different concentrations.**

The reasons are attributed to three points, as shown in Figure 6c, d and Figure 7b. The first one is the small difference between excited green emission from 1% QDs and 2% QDs. Second, a large amount of blue light can pass through the 12.5% KSF film and excite the QDs film in QDs-up type. Finally, the reflectance rate of 35% KSF film to green light is much higher in QDs-down type.

Because of the strong absorption from QDs, there is only a little blue light which excite the KSF in QDs- down type. Without the block of QDs film, KSF film absorb more blue light in QDs-up type, and its optical power of red emission is 44.71% higher than that of the QDs-down type at 50 mA (Figure 5c). As a result, the whole optical power of QDs-up type is 13.83 mW, 24.26% higher than that of the QDs-down type at 50 mA (Figure 5d). Besides, the luminous efficiency of QDs-up type and QDs-down type is 13.54 lm/W and 10.77 lm/W, which means the former is 25.72% higher.

In addition, CCE is defined as the ratio between excited emission and absorbed emission, which can be calculated as following:

$$\mathrm{CCE} = (\mathrm{P_{G\_em}} + \mathrm{P_{R\_em}})/(\mathrm{P_{B\_ex}} - \mathrm{P_{B\_em}}), \qquad (4)$$

where $\mathrm{P_{B\_ex}}$ is the excitation power of the blue LED. The higher CCE is, the more excited emission attained at the same current. The CCEs of the two types WLEDs, LED devices without KSF film, and that without QDs film at 50 mA or at 150 mA were calculated. As shown in Figure 6a and b, the CCE of the QDs-up type is higher than that of the QDs-down type. When the supply current is 50 mA, the CCEs of the QDs-up type and QDs-down type are 11.94% and 9.29%, respectively, and those are 17.78%, 13.69% at 150 mA.

The CCEs of the QDs and KSF films were also calculated, as shown in 6c and d. The CCEs of the QDs and KSF films used in the QDs-up type are both lower than that of the QDs-down type, which means the films with lower efficiency combine the WLEDs with a higher CCE. The QDs have a much stronger absorption, and CCEs of KSF films are higher than those of the QDs films. Therefore, the location of KSF film below can avoid the too much absorption of QDs, results in a higher conversion efficiency in QDs-up type. Although the CCE of 35% KSF film in QDs-down type is twice as high as that of 12.5% KSF film, most of the blue light is absorbed by 1% QDs film and the influence of KSF film is weakened.

To further explain the optical power and luminous efficiency differences between two types, the reflectance rate and absorption rate of QDs and KSF films with different concentrations were also measured in details. Figure 7a and b shows that the QDs films and 35% KSF film mainly reflect the light with wavelength longer than 500 nm, and the reflection of 12.5% KSF film is lower at different wavelengths. Figure 7c and d shows that the strong absorption source of these films is blue LED. For QDs-up type, the reflection and absorption rate of 12.5% KSF film to blue light is low, so the green emission from 2% QDs film is enough. The reflectance and absorption rate of 2% QDs imply that the transmittance rate to red emission is over 50%. For QDs-down type, the strong absorption of 1% QDs film leads to the lower red emission, and the blue emission is weakened

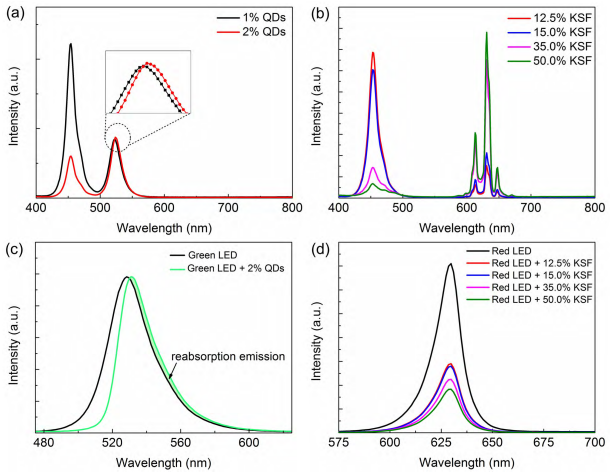

FIGURE 8. (a) Emission spectra of LED devices composed by blue LED and QDs. (b) Emission spectra of LED devices composed by blue LED and KSF. (c) Normalized emission spectra of green LED and of green LED with QDs. (d) Normalized emission spectra of red LED and of red LED with KSF.

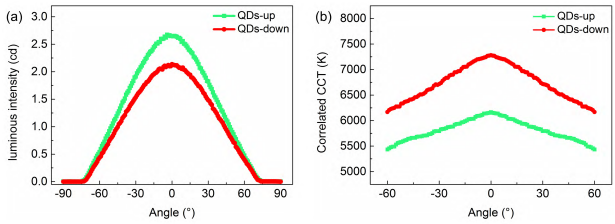

FIGURE 9. (a) Angular dependent luminous intensity of QDs-up type and QDs-down type WLEDs. (b) Angular dependent CCT of QDs-up type and QDs-down type WLEDs.

by the strong absorption of 35% KSF film. Therefore, the QDs-up type has a higher optical power and luminous efficiency.

In addition to intensity, the peak position is also important in emission spectra. Figure 4 shows the peaks of the blue and red emissions are located at 453, 613, 631 and 648 nm. However, the peak of green emission appears at 522 nm in QDs-up type and at 525 nm in QDs-down type. To find out the reasons of peak position change, the emission spectra of LED devices composed of blue LED and QDs films, or that composed of blue LED and KSF films were also collected. As shown in Figure 8a and b. the red shift of green emission also appears in the LED devices contained QDs films, but not for the KSF films. To explain this red shift, the emission spectra of the green LED, green LED with QDs film, red LED and red LED with KSF films were obtained. In Figure 8c, after the addition of QDs film, a part of the light from the green LED is absorbed by QDs and the added emission appears. The peak location changes from 529 nm to 531 nm. But for the red LED with KSF films, the peaks maintain at 630 nm, as shown in Figure 8d. Combined these findings with the overlapping between absorption and PL spectra of QDs (Figure 2), it can be learned that the red shift of green emission is a result from the reabsorption of QDs [31], [32]

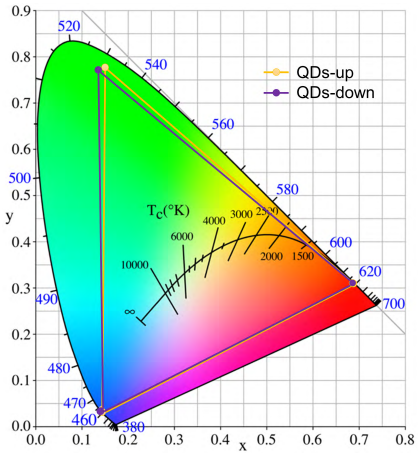

FIGURE 10. Chromaticity coordinates of blue emission, green emission and red emission in QDs-up type and QDs-down type WLEDs.

The results above are the overall optical properties of the device, but the properties changes with the spatial position is equally important. For comparing the spatial distribution of luminous intensity and CCT, the angular dependent measurements were used, as shown in Figure 9. Because the blue LED is a Lambertian emitter, all of the maximum intensity and CCT appear in the middle, and the minimum one is in the margin. At the angle of 0°, the luminous intensity of QDs-up type and QDs-down type is 2.65 and 2.14 cd, respectively. The higher luminous intensity of QDs-up type also indicates its higher optical power.

As representing the color component contained in the light, CCT is another focus point for the backlight and display. To compare the CCT spatial distribution, ΔCCT is defined as the CCT difference between the middle and the margin. As shown in Figure 9b, the ΔCCT of QDs-down type and QDs-up type is 1112K and 734K. This suggests that CCT uniformity at different angles of the QDs-up type is much better. As reported in the article, the CCT shift is a problem that cannot to be ignored for QDs, and the shift is affected by the emission ratio from QDs [33], [34] From Figure 6a, the green emission ratio of QDs-down type and QDs-up type is 34.8% and 40.1%, which implies the CCT shift of former is more obvious.

The chromaticity coordinates of three emissions and the color gamut of two types WLEDs were obtained, as shown in Figure 10. The chromaticity coordinates of blue emission and red emission are the same, (0.147,0.032) and (0.689,0.311), respectively. But the coordinates of green emission are different, (0.151, 0.775) for QDs-up type and (0.136,0.773) for QDs-down type, corresponding to its red shift of peak location. The coordinates of three emissions consist of a triangle, and the area of that triangle is the color gamut. The color gamut of QDs-up type is 126.9% National Television Standards Committee (NTSC) and that of QDs-down type is 127.1% NTSC. It indicates that both of these WLEDs have a large color gamut, and the QDs have an advantage on backlight and display rather than traditional green phosphor.

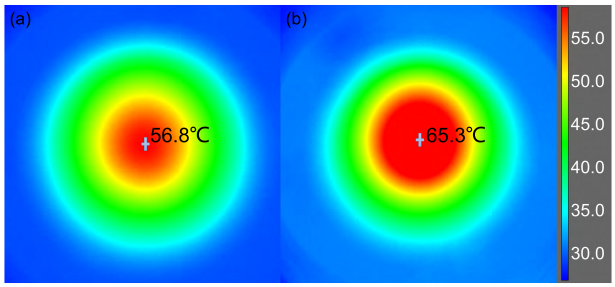

FIGURE 11. (a) Infrared thermal image of QDs-up type WLEDs. (b) Infrared thermal image of QDs-down type WLEDs.

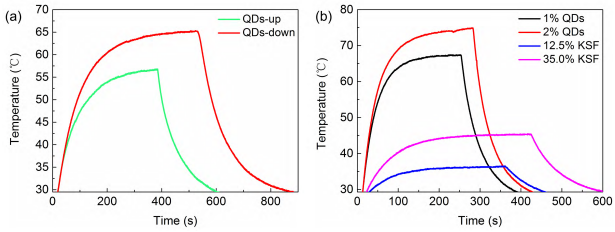

FIGURE 12. (a) The highest temperature curves of QDs-up type and QDs-down type WLEDs over time. (b) The highest temperature curves of LED devices composed by blue LED and QDs, and that composed by blue LED and KSF.

C. COMPARISON OF THERMAL PROPERTIES BETWEEN QDs-up TYPE AND QDs-down TYPE

In addition to optical properties, the thermal properties are also an important concern for WLEDs, because higher temperature leads to the quenching and degradation of QDs or KSF [29], [35]. To explore the temperature distribution of the WLEDs, we recorded the infrared thermal images of two types at 50 mA from switching to closing. When the temperature tends to be stable, the thermal images were collected (Figure 11), and the power supply was stopped. In Figure 11, the highest temperature T_{max} of QDs-down type is 65.3°, 14.9% higher than that of the QDs-up type. The QDs-down type has a larger area with temperature over 50°. For comparing the heating and cooling times, the highest temperature curves were measured, as Figure 12a shown. For the QDs-up type, it takes 170s when heated from environmental temperature to 90% T_{max}, and takes 154s when cooled from T_{max} to 10% T_{max}. However, all of these are 201 and 209s for the QDs-down type, which means the heat-transfer speed of QDs-up type is higher.

To find out why the thermal properties of the QDs-down type are worse than those of the QDs-up type, the temperature curves of LED devices composed of blue LED and QDs film, or composed of blue LED and KSF film were measured. In Figure 12b, the T_{max} of devices assemblies of 1% QDs, 2% QDs, 12.5% KSF and 35% KSF films is 67.4°, 74.9°, 36.7° and 45.4°, respectively. Because the QDs films have a lower CCE, a large amount of luminous energy from blue LED transform into the heat. For QDs-down type, the actual green emission is more than the measured one because of the reflection from KSF film, and the position below is not conducive for QDs films to have a heat dissipation. Thus, the heat of QDs film in QDs-down type is more than that in QDs-up type.

TABLE 2. Optical and thermal properties comparison of two types WLEDs at 50 mA.

Name	QDs-up type	QDs-down type
Concentrations of QDs	2%	1%
Concentrations of KSF	12.5%	35%
Chromaticity coordinate (x)	0.3245	0.3466
Chromaticity coordinate (y)	0.3089	0.3372
Optical Power (mW)	13.83	11.13
Luminous efficiency (lm/W)	13.54	10.77
CCE	11.94%	9.29%
Luminous Intensity Maximum (cd)	2.65	2.14
ΔCCT (K)	734	1112
Color Gamut (NTSC)	126.9%	127.1%
T_{max} (℃)	56.8	65.3

Based on the discussion above, the main optical and thermal properties at 50 mA are compared in Table 2. The QDs-up type has a higher optical power of 24.26%, and a higher luminous efficiency of 25.72%, an increased CCE of 2.63%, a higher luminous intensity of 23.83%, a lower ΔCCT of 51.5% and a decreased T_{max} of 14.9%. These results further demonstrate that the QDs film located above is more beneficial to the color conversion, CCT uniformity and heat dissipation, and the QDs-up type is more suitable for the backlight and display.

IV. CONCLUSION

In summary, the optical and thermal properties of the QDs-up type and QDs-down type WLEDs with different layers location are systematically studied. By changing the concentration of QDs and KSF, the two types WLEDs with similar chromaticity coordinates were first prepared. The optical power, luminous efficiency, CCE and luminous intensity in the middle of QDs-up type are 13.83 mW, 13.54 lm/W, 11.94% and 2.65 cd, meaning 24.26%, 25.72%, 2.63% and 23.83% higher than those of QDs-down type, respectively. Besides, the ΔCCT and T_{max} of QDs-up type are 734 K and 56.8°, respectively (51.5% and 14.9% lower). With the spectra, CCE, reflection rate, absorption rate and temperature analysis of QDs or KSF films, the KSF films located below can decrease the emission loss, increase the color uniformity of spatial distribution and enhance the heat dissipation for WLEDs. These results demonstrate that the QDs-up type WLEDs has a better optical and thermal properties, and are more suitable for the application to backlight and display.

REFERENCES

[1] D. A. Steigerwald, J. C. Bhat, D. Collins, R. M. Fletcher, M. O. Holcomb, M. J. Ludowise, P. S. Martin, and S. L. Rudaz, "Illumination with solid state lighting technology," *IEEE J. Sel. Topics Quantum Electron.*, vol. 8, no. 2, pp. 310–320, Mar./Apr. 2002.

[2] E. F. Schubert, J. K. Kim, H. Luo, and J.-Q. Xi, "Solid-state lighting—A benevolent technology," *Rep. Prog. Phys.*, vol. 69, no. 12, pp. 3069–3099, 2006.

[3] K. Lu, W. Zhang, and B. Sun, "Multidimensional data-driven life prediction method for white LEDs based on BP-NN and improved-adaboost algorithm," *IEEE Access*, vol. 5, pp. 21660–21668, 2017.
[4] F. Jin, X. Li, R. Zhang, C. Dong, and L. Hanzo, "Resource allocation under delay-guarantee constraints for visible-light communication," *IEEE Access*, vol. 14, pp. 1020–1034, 2016.
[5] N. C. George, K. A. Denault, and R. Seshadri, "Phosphors for solid-state white lighting," *Annu. Rev. Mater. Res.*, vol. 43, pp. 481–501, Jul. 2013.
[6] T. Ogi, A. B. D. Nandiyanto, K. Okino, F. Iskandar, W.-N. Wang, E. Tanabe, and K. Okuyama, "Towards better phosphor design: Effect of SiO_2 nanoparticles on photoluminescence enhancement of YAG:Ce," *ECS J. Solid State Sci. Technol.*, vol. 2, pp. R91–R95, 2013.
[7] A. Purwanto, W.-N. Wang, I. W. Lenggoro, and K. Okuyama, "Formation and luminescence enhancement of agglomerate-free YAG: Ce submicrometer particles by flame-assisted spray pyrolysis," *J. Electrochem. Soc.*, vol. 154, no. 3, pp. J91–J96, May 2007.
[8] C. F. Lai, J. S. Li, and C. W. Shen, "High-efficiency robust free-standing composited phosphor films with 2D and 3D nanostructures for high-power remote white LEDs," *ACS Appl. Mater. Inter.*, vol. 9, pp. 4851–4859, Feb. 2017.
[9] T. Güner, U. Şentürk, and M. M. Demir, "Optical enhancement of phosphor-converted wLEDs using glass beads," *Opt. Mater.*, vol. 72, pp. 769–774, Oct. 2017.
[10] T. Erdem and H. V. Demir, "Color science of nanocrystal quantum dots for lighting and displays," *Nanophotonics*, vol. 2, no. 1, pp. 57–81, 2013.
[11] S. Ananthakumar, J. R. Kumar, and S. M. Babu, "Cesium lead halide (CsPbX3, X=Cl, Br, I) perovskite quantum dots-synthesis, properties, and applications: A review of their present status," *J Photon. Energy*, vol. 6, Oct. 2016, Art. no. 042001.
[12] X. He, Y. Qiu, and S. Yang, "Fully-inorganic trihalide perovskite nanocrystals: A new research frontier of optoelectronic materials," *Adv. Mater.*, vol. 29, no. 32, Aug. 2017, Art. no. 1700775.
[13] S. Sun, D. Yuan, Y. Xu, A. Wang, and Z. Deng, "Ligand-mediated synthesis of shape-controlled cesium lead halide perovskite nanocrystals via reprecipitation process at room temperature," *ACS Nano*, vol. 10, no. 3, pp. 3648–3657, Mar. 2016.
[14] L. Rao, Y. Tang, C. Song, K. Xu, E. T. Vickers, and S. B. Naghadeh, "Polar-solvent-free synthesis of highly photoluminescent and stable $CsPbBr_3$ nanocrystals with controlled shape and size by ultrasonication," *Chem. Mater.*, vol. 31, no. 2, pp. 365–375, Dec. 2018.
[15] N. S. Makarov, S. Guo, O. Isaienko, W. Liu, I. Robel, and V. I. Klimov, "Spectral and dynamical properties of single excitons, biexcitons, and trions in cesium–lead-halide perovskite quantum dots," *Nano Lett.*, vol. 16, no. 4, pp. 2349–2362, Apr. 2016.
[16] D. Wang, D. Wu, D. Dong, W. Chen, J. Hao, and J. Qin, "Polarized emission from $CsPbX_3$ perovskite quantum dots," *Nanoscsle*, vol. 8, no. 22, pp. 11565–11570, Jun. 2016.
[17] L. Rao, X. Ding, X. Du, G. Liang, Y. Tang, and K. Tang, "Ultrasonication-assisted synthesis of CsPbBr3 and Cs4PbBr6 perovskite nanocrystals and their reversible transformation," *Beilstein J. Nanotechnol.*, vol. 10, pp. 666–676, Feb. 2019.
[18] X. Li, Y. Wu, S. Zhang, B. Cai, Y. Gu, and J. Song, "$CsPbX_3$ quantum dots for lighting and displays: Room-temperature synthesis, photoluminescence superiorities, underlying origins and white light-emitting diodes," *Adv. Funct. Mater.*, vol. 26, no. 15, pp. 2435–2445, Apr. 2016.
[19] M. Meyns, M. Perálvarez, A. Heuer-Jungemann, W. Hertog, M. Ibáñez, R. Nafria, A. Genç, J. Arbiol, M. V. Kovalenko, J. Carreras, A. Cabot, and A. G. Kanaras, "Polymer-enhanced stability of inorganic perovskite nanocrystals and their application in color conversion LEDs," *ACS Appl. Mater. Inter.*, vol. 8, no. 30, pp. 19579–19586, Jul. 2016.
[20] Y. Wei, X. Deng, Z. Xie, X. Cai, S. Liang, P. A. Ma, Z. Hou, Z. Cheng, and J. Lin, "Enhancing the stability of perovskite quantum dots by encapsulation in crosslinked polystyrene beads via a swelling–shrinking strategy toward superior water resistance," *Adv. Funct. Mater.*, vol. 27, no. 39, Oct. 2017, Art. no. 1703535.
[21] J. De Roo, M. Ibanez, P. Geiregat, G. Nedelcu, W. Walravens, and J. Maes, "Highly dynamic ligand binding and light absorption coefficient of cesium lead bromide perovskite nanocrystals," *ACS Nano*, vol. 10, no. 2, pp. 2071–2081, Feb. 2016.
[22] J. Li, L. Xu, T. Wang, J. Song, J. Chen, J. Xue, Y. Dong, B. Cai, Q. Shan, B. Han, and H. Zeng, "50-fold EQE improvement up to 6.27% of solution-processed all-inorganic perovskite $CsPbBr_3$ QLEDs via surface ligand density control," *Adv. Mater.*, vol. 29, no. 5, Feb. 2017, Art. no. 1603885.
[23] C. C. Lin and R.-S. Liu, "Advances in phosphors for light-emitting diodes," *J. Phys. Chem. Lett.*, vol. 2, no. 11, pp. 1268–1277, May 2011.
[24] S. Chanyawadee, P. G. Lagoudakis, R. T. Harley, M. D. B. Charlton, D. V. Talapin, H. W. Huang, and C.-H. Lin, "Increased color-conversion efficiency in hybrid light-emitting diodes utilizing non-radiative energy transfer," *Adv. Mater.*, vol. 22, no. 5, pp. 602–606, Feb. 2010.
[25] T. Fukui, K. Kamon, J. Takeshita, H. Hayashi, T. Miyachi, Y. Uchida, S. Kurai, and T. Taguchi, "Superior illuminant characteristics of color rendering and luminous efficacy in multilayered phosphor conversion white light sources excited by near-ultraviolet light-emitting diodes," *Jpn. J. Appl. Phys.*, vol. 48, no. 1, 2009, Art. no. 112101.
[26] Y. Zhu and N. Narendran, "Investigation of remote-phosphor white light-emitting diodes with multi-phosphor layers," *Jpn. J. Appl. Phys.*, vol. 49, Oct. 2010, Art. no. 100203.
[27] C.-H. Chiang, H.-Y. Tsai, T.-S. Zhan, H.-Y. Lin, Y.-C. Fang, and S.-Y. Chu, "Effects of phosphor distribution and step-index remote configuration on the performance of white light-emitting diodes," *Opt. Lett.*, vol. 40, no. 12, pp. 2830–2833, 2015.
[28] B. Xie, W. Chen, J. Hao, D. Wu, X. Yu, Y. Chen, R. Hu, K. Wang, and X. Luo, "Structural optimization for remote white light-emitting diodes with quantum dots and phosphor: Packaging sequence matters," *Opt. Express*, vol. 24, pp. A1560–A1570, Dec. 2016.
[29] J.-S. Li, Y. Tang, Z.-T. Li, X.-R. Ding, L.-S. Rao, and B.-H. Yu, "Effect of quantum dot scattering and absorption on the optical performance of white light-emitting diodes," *IEEE Trans. Electron Devices*, vol. 65, no. 7, pp. 2877–2884, Jul. 2018.
[30] Y. Tang, H. Lu, L. Rao, Z. Li, X. Ding, C. Yan, and B. Yu, "Regulating the emission spectrum of $CsPbBr_3$ from green to blue via controlling the temperature and velocity of microchannel reactor," *Materials*, vol. 11, no. 3, p. 371, Mar. 2018.
[31] M. A. Koc, S. N. Raja, L. A. Hanson, S. C. Nguyen, N. J. Borys, A. S. Powers, S. Wu, K. Takano, J. K. Swabeck, J. K. Swabeck, J. H. Olshansky, L. Lin, R. O. Ritchie, and A. P. Alivisatos, "Characterizing photon reabsorption in quantum dot-polymer composites for use as displacement sensors," *ACS Nano*, vol. 11, no. '2, pp. 2075–2084, Jan. 2017.
[32] I. Coropceanu and M. G. Bawendi, "Core/shell quantum dot based luminescent solar concentrators with reduced reabsorption and enhanced efficiency," *Nano Lett.*, vol. 14, no. 7, pp. 4097–4101, Jun. 2014.
[33] K.-J. Chen, C.-C. Lin, H.-V. Han, C.-Y. Lee, S.-H. Chien, K.-Y. Wang, S.-H. Chiu, Z.-Y. Tu, J.-R. Li, T.-M. Chen, X. Li, M.-H. Shih, H.-C. Kuo, and W. Kuan-Yu, "Wide-range correlated color temperature light generation from resonant cavity hybrid quantum dot light-emitting diodes," *IEEE J. Sel. Topics Quantum Electron.*, vol. 21, no. 4, Jul./Aug. 2015, Art. no. 1900407.
[34] Y. Tang, Z. Li, Z.-T. Li, J.-S. Li, S.-D. Yu, and L.-S. Rao, "Enhancement of luminous efficiency and uniformity of CCT for quantum dot-converted LEDs by incorporating with ZnO nanoparticles," *IEEE Trans. Electron Devices*, vol. 65, no. 1, pp. 158–164, Jan. 2018.
[35] Y. Zhao, F. Yun, L. Feng, S. Wang, Y. Li, X. Su, M. Guo, W. Ding, and Y. Zhang, "Improving peak-wavelength method to measure junction temperature by dual-wavelength LEDs," *IEEE Access*, vol. 5, pp. 11712–11716, 2017.